

## Effect of Irradiation with DC Plasma Jet on the Structure Phase Compositions and Properties of Powder Ni and Co – based Coatings

Darya ALONTSEVA<sup>1\*</sup>, Alexander KRASAVIN<sup>1</sup>, Alyona RUSSAKOVA<sup>1,2</sup>,  
Tatyana KOLESNIKOVA<sup>1</sup>, Gulsym BEKTASOVA<sup>3</sup>

<sup>1</sup> East-Kazakhstan State Technical University, Ust-Kamenogorsk, 69 Protazanov St., 070004, Kazakhstan

<sup>2</sup> Eurasian National University, Astana, 5 Munaypasov St., 010000, Kazakhstan

<sup>3</sup> East-Kazakhstan State University, 34 30<sup>th</sup> Gvardeyskya St., Ust-Kamenogorsk, 070004 Kazakhstan

crossref <http://dx.doi.org/10.5755/j01.ms.22.2.7699>

Received 31 July 2014; accepted 12 February 2015

This paper presents new results of transmission electron microscopy (TEM), scanning electron microscopy (SEM), X-ray diffraction (XRD) and atomic force microscopy (AFM) investigation of the structure-phase compositions of coatings on the base of Ni and Co deposited by plasma-detonation on steel substrates after their modification by DC plasma jet irradiation. The phase structures and morphology of precipitation of strengthening phases from solid solution are defined. The irradiation of the coatings leads to the evolution of the structural-phase state of coatings: an increase in the size of the diffusion zone between the coating and the substrate, an increase in the volume fraction of hardening intermetallic phases, the formation of sufficiently homogeneous fine-grained structure in the irradiated coatings and, consequently, a significant increase of hardness, corrosion and wear resistance of modified coatings. There is a mutual penetration of the substrate main element Fe in the coating and base coating elements (Ni and Co correspondingly) into the substrate as a result of the coating treatment by a pulse DC plasma jet.

**Keywords:** structure-phase composition, plasma-detonation coatings, morphology of precipitation, wear resistance, corrosion resistance, radiation-enhanced diffusion.

### 1. INTRODUCTION

The protective powder Ni and Co based coatings produced by the methods of Thermal Coating Spraying, High Velocity Oxy-Fuel (HVOF) coating spraying or plasma detonation designed for the protection of surfaces of industrial products working at high temperatures and in corrosive environments (cylinder liners, cervical shaft gas turbine engine compressor stators, the details of construction of pipelines, etc) [1–7]. It is known that Ni-based alloys have good properties for corrosion protection at high temperature [8–10]. Co improves the heat resistance of the alloys, as well as their wear resistance and hardness at high temperatures [8, 11, 12]. To homogenize the structure of powder coatings produced by plasma detonation additional treatment by plasma jet or electron beam, or laser heat treating are applied [2, 4, 5, 13]. The plasma detonated Ni and Co-based coatings have an fcc lattice [14–17], which provides some technological advantages. Particularly, the alloys with the fcc lattice have higher welding properties and better endurance capability at high temperatures. Their grains are unlikely to increase during heating, and retain ductility at low temperatures [12]. Previously, we have carried out model calculations of temperature distribution in the two-layer absorbers heated by a moving source; on their basis were given recommendations on exposure modes, presumably to ensure certain temperature profiles, acceleration of diffusion processes and the precipitation of certain phases

in the protective powder coatings deposited by a plasma jet on steel substrate [14, 17].

We have experimentally established that the hardening in the material provided by the precipitation of intermetallic compounds [14–17], which are known to retain their structure and properties at high temperatures [18, 19]. The form of strengthening nanoparticles precipitation from a solid solution is determined by thermodynamical efficiency due to the type of dissolution of the supersaturated solid solution in nonequilibrium conditions (high temperature, deformation, irradiation) [20]. It is known that the form of intermetallic particles can affect the strength and corrosion properties of the material [20–22]. Thus, determination of the morphology of the strengthening particles precipitated from the solid solution upon irradiation has a great scientific and practical value. Due to acceleration of the diffusion processes under irradiation [23], the irradiation can also be used to improve the adhesion of coatings to the substrate and, accordingly, to increase their wear resistance and corrosion resistance.

The aim of this research is to establish the regularities of the evolution of structural and phase composition and properties of Ni and Co based powder coatings as a result of their additional treatment by DC pulse plasma jet, experimentally verify predictions about the behavior of these materials under irradiation.

### 2. EXPERIMENTAL DETAILS

150–300 μm thick protective coatings were deposited on a steel substrate with an “Impulse-6” plasma detonation unit. The substrate material was Steel 3 (Fe–base, C–0.25 %, Mn–0.8 %, Si–0.37 %, P < 0.045 %). For the

Corresponding author. Tel.: +723-254-0586; fax: +723-226-4709.  
E-mail address: [dalontseva@mail.ru](mailto:dalontseva@mail.ru) (D. Alontseva)

coatings we used the AN-35 Co-based powder alloy with additives of Cr (8–32 %); Ni ( $\leq 3$  %), Si (1.7–2.5 %), Fe ( $\leq 3$  %); C (1.3–1.7 %) and W (4–5 %) and the PG-19N-01 Ni-based powders alloy with additives of Cr (8–14 %), B (2.3 %), Si (1.2–3.2 %), Fe (5 %), C (0.5 %) (Russian Industrial Standard). The powder fractions varied in size from 56 to 260  $\mu\text{m}$ . The powder coatings were deposited in air according to the following mode: 60 mm distance from the sample to the plasma jet nozzle edge; 360 mm/min velocity of the sample; 4 Hz pulse frequency. The density of plasma jet electric current fluctuates from 1 to 7  $\text{A}/\text{cm}^2$ ; the rate of heat transfer in the sample varies in the  $q = (0.1 - 5) \cdot 10^6 \text{ W}/\text{cm}^2$  as it depends on the density of electric current. The temperature of the plasma flow at the nozzle exit in average makes about several thousand  $^\circ\text{C}$ . The average plasma jet size across the sample is 25 mm; the pulse elapsed time is about 10  $\mu\text{s}$ . Propane, oxygen and air were used for combustion, and Mo was adopted as a plasma-jet eroding electrode material.

The deposition of coatings and additional irradiation treatment were carried out at the Sumy Institute for Surface Modification (Sumy, Ukraine). The selection of the additional exposure modes is based on modeling of temperature profiles in the coatings and the substrate during irradiation [12, 14–17]. We picked out such modes of irradiation at which on the surface the Ni or the Co melting temperature is achieved, and on the border between the coating and the substrate the temperature is high enough to significantly accelerate the diffusion processes and to increase the width of the diffusion zone from the coating to the substrate, but not to lead to coating full melting. The optimal modes were thought those that would lead to homogenization of the coating and improve its adhesion to the substrate due to the acceleration of diffusion processes during irradiation.

The following modes of additional irradiation were applied using DC pulse plasma jet: plasma jet power density of  $1.9 \times 10^9 \text{ W}/\text{m}^2$ ; pulse elapsed time of  $3 \times 10^{-6} \text{ sec}$ ; pulse frequency of 2.5 Hz; the samples are irradiated in air.

Experimental methods of analysis included Transmission Electron Microscopy (TEM) and Scanning Transmission Electron Microscopy (STEM) with Energy Dispersive Spectrometry (EDS) by JEM-2100 (“JEOL”, Japan) and by TECNAI, (Phillips), X-ray diffraction (XRD) by X’Pert PRO (“PANalytical”, the Netherlands), Scanning Election Microscopy (SEM) by JSM-6390LV (“JEOL”, Japan) with EDS (“Oxford Instruments”, Great Britain), Atomic Force Microscopy (AFM) by NT-206 (Belorussia).

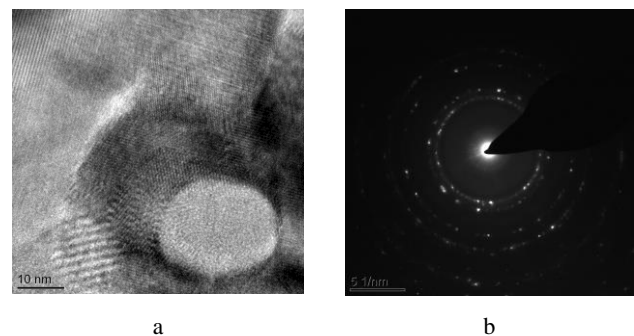
Interpretation of X-ray diffraction patterns was carried out using the license data PCP DFWIN (140,000

compounds) and Diffracts Plus, ASTM catalogs. M-691 Precision Ion Polishing System (“Gatan”, USA) was used to prepare TEM foils by the Ar ion sputter etching method. Surface topography of the coatings was examined also using a scanning probe microscope SmartSPM (“AIST-NT”, Russia). The morphology and structure of the strengthening nanoparticles and their volumetric fraction in the material was determined by TEM. We used the CrystalMarker software application and comparison with TEM data on structural and phase composition obtained by X-ray diffraction phase analysis.

Microhardness test of the samples was performed on a digital microhardness LM-700 (LECO, Russia). Load on the indenter was 2.3 N. Exposure time was 5 seconds. Wearability was measured with a SMTS-2 (“Selmi”, Ukraine) using a plane-cylinder scheme in technical petroleum jelly. Corrosion was tested using the potentiostatic method to measure the sea-water corrosion rate. The experiment of removing polarization curves was carried out with a PI-50.1.1 potentiostat (“ElectroTechSnab”, Russia).

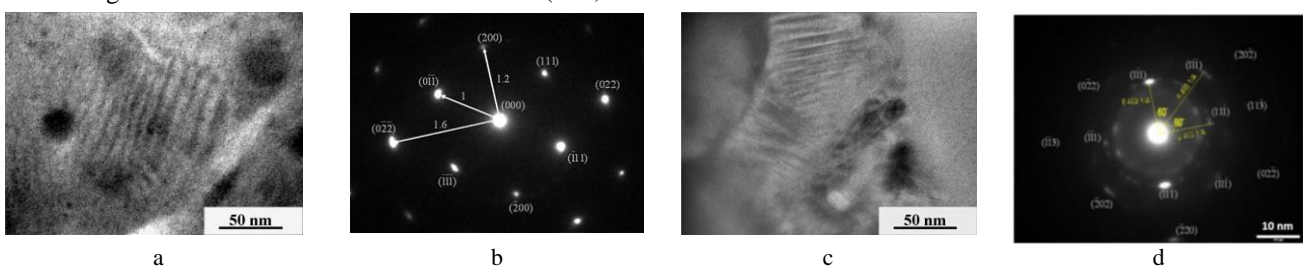
### 3. RESULTS AND DISCUSSION

Fig. 1 shows the TEM-images of Ni-based irradiated coating and the typical polycrystalline ring diffraction pattern. The base through-thickness layer of coatings is a mixture of crystallographically differently oriented nanograins. These results are in a good agreement with the data of X-ray analysis. X-ray nickel diffraction peaks are expanded and their amplitudes are reduced. We have established the type of crystal lattice (it is fcc) and its parameter  $a = 3.53 \text{ \AA}$ . Thus, the matrix structure of the coating after irradiation is not changed [13, 14].



**Fig. 1.** TEM images: a – Ni-based irradiated coatings; b – corresponding diffraction pattern

The phase structures and morphology of precipitation of strengthening phases from solid solution are defined by TEM methods (Fig. 2). It was established that  $\text{CrNi}_3$  phase with the fcc type of crystal lattice precipitated in the



**Fig. 2.** TEM images of the irradiated coatings: a – AN-35 – the  $\text{Co}_{0.8}\text{Cr}_{0.2}$  particles, b – and their diffraction pattern; c – PG-19N-01 – the  $\text{CrNi}_3$  particles; d – and their diffraction pattern

Ni-based coatings, and  $\text{Co}_{0.8}\text{Cr}_{0.2}$  phase with the hcp type of crystal lattice precipitated in Co-based coatings. Both phases are allocated in the form of lamellas up to 50 nm long and 5 nm in diameter (Fig. 2). These nanosize intermetallic phases were observed in these coatings before irradiation and were deemed strengthening as the greatest microhardness of a coating corresponded to those places where the volume concentration of these phases was highest [14–17]. It was established by TEM and XRD methods that the volume concentration of these phases in the coatings increased in average by 5 % after irradiation (Fig. 3). Correspondingly, an increase in microhardness was observed (Fig. 4). It is also noted that the volume fractions of Co-based and Ni-based solid solution with the fcc lattice increase (Fig. 3). Mo appears on the surface of a coating after irradiation under the estimated regimes (Fig. 3). It is particularly important that there is a transition (diffusion) zone between the coating and the substrate, where the compounds of Co or Ni with Fe evolve. The width of the diffusion zone for the samples before irradiation is estimated in average as 100 micron: 50 micron in the coating and 50 micron in the substrate (by processing the data on the distribution of microhardness across the depth from the surface, and according to the X-ray phase analysis data). The size of the diffusion zone between the coating and the substrate after irradiation increased in average by 2 times (Fig. 4). Using TEM with Energy Dispersive X-Ray analysis (EDX) we obtained the EDX spectra (Fig. 5). Using STEM with EDS we obtained the map of element distribution in the foil of the Ni-based coating (Fig. 6).

The maps show the presence of such elements as Ni, Cr, Fe, Al similarly to their peaks presence in EDX spectrum (Fig. 5) and also Mo presences here (Fig. 6). It is evident that Mo penetrates into the surface from the Mo electrode. Al was present in the coatings before irradiation [15,16]. Probably the samples were polluted in the chamber in the process of coating deposition.

SEM with EDS also registers the penetration of Ni from the irradiated Ni-based coatings into the substrate and the penetration of Co from the irradiated Co-based coatings into the substrate as well as penetration of Fe from the substrate into the irradiated coatings (Fig. 7 and [14]).

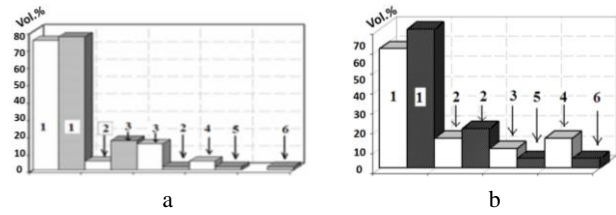
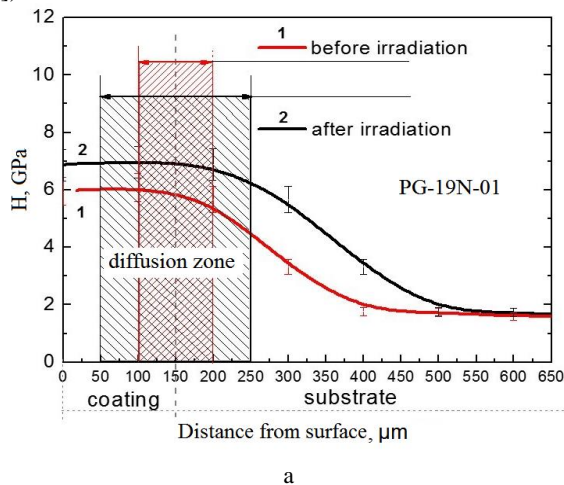


**Fig. 3.** Comparison of phase coating compositions before (light bar) and after (dark bar) irradiation: a–for PG-19N-01: 1–Ni; 2– $\text{Cr}_{13}\text{Ni}_5\text{Si}_2$ ; 3– $\text{CrNi}_3$ ; 4– $\text{NiO}$ ; 5– $\text{Fe}_7\text{Ni}_3$ ; 6– $\text{Mo}_2\text{C}$ ; b–for AN 35: 1–Co; 2– $\text{Co}_{0.8}\text{Cr}_{0.2}$ ; 3– $\text{FeCr}_2\text{O}_4$ ; 4– $\text{CoCr}_2\text{O}_4$ ; 5–CoFe; 6–Mo; Cubic, Pm-3m and  $\text{MoO}_3$

The Ni and Co depth of penetration into the substrate makes more than 100 microns. We suggested development of radiation-enhanced diffusion in the absorbing materials during irradiation; but without experimental measurement of diffusion coefficients we are unable to predetermine the contribution of one or another factor in the acceleration of mass transfer, except that by circumstantial evidence. However our results are in good agreement with the data of other authors who note the radiation-enhanced diffusion in materials with an fcc lattice during irradiation, leading to heating up to the temperatures we specified [23]. The microstructure of the coatings after irradiation is the fine-grained homogeneous microstructure with an average grain size of 2 microns (Fig. 7).

After irradiation PG-19N-01 coating is resistant to corrosion in sea water. Steel 3 substrate and PG-19N-01 coating sea water corrosion potential is rather high:  $\varphi_{\text{corr}} = -0.38 \text{ V}$  and  $\varphi_{\text{corr}} = -0.49 \text{ V}$  correspondingly. Yet the substrate corrosion rate is considerably higher:  $i_{\text{corr}}(\text{substrate}) = 3.7 \text{ mm/yr}$ ,  $i_{\text{corr}}(\text{coating}) = 2.2 \text{ mm/yr}$ .

The roughness decreases in average by 2 times (from  $R_a = 0.1072 \mu\text{m}$  to  $R_a = 0.0535 \mu\text{m}$  for Ni-based coating and from  $R_a = 0.20 \mu\text{m}$  to  $R_a = 0.10 \mu\text{m}$  for Co-based coating) at the expense of melting the coating surface, which corresponds to the specified temperatures at the surface of the coating. As a result of the coatings' modification by irradiation their wear resistance increased by up to 2–3 times (Fig. 8).

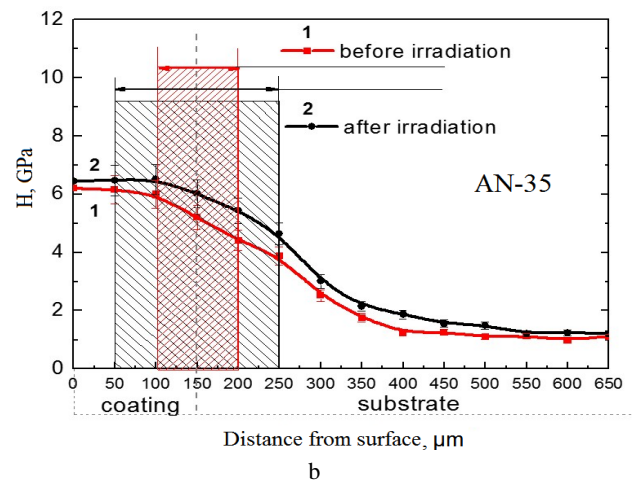


**Fig. 4.** The curves of distribution of microhardness in the PG-19N-01 and AN-35 coating in depth from the surface before and after irradiation

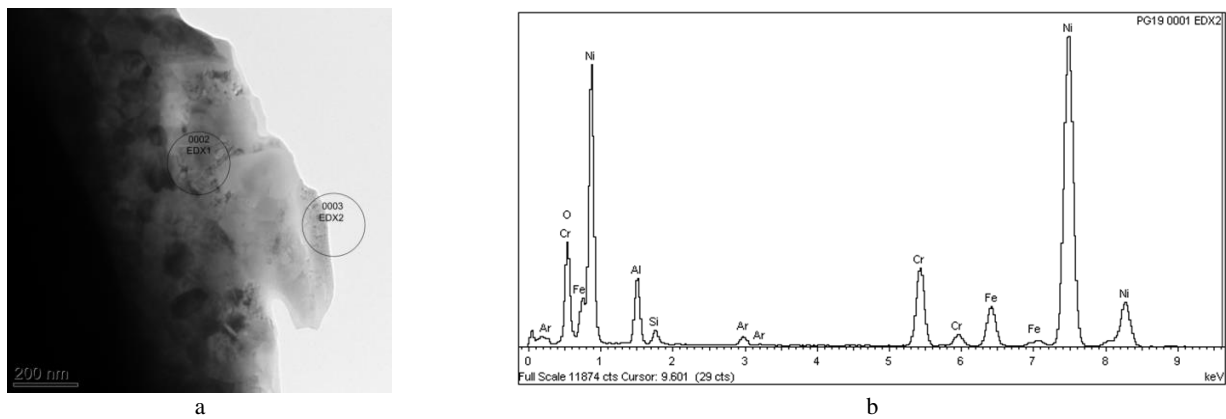


**Fig. 5.** TEM image of Ni-based coating: a – the area for which the EDX analyses have been made; b – EDX spectrum

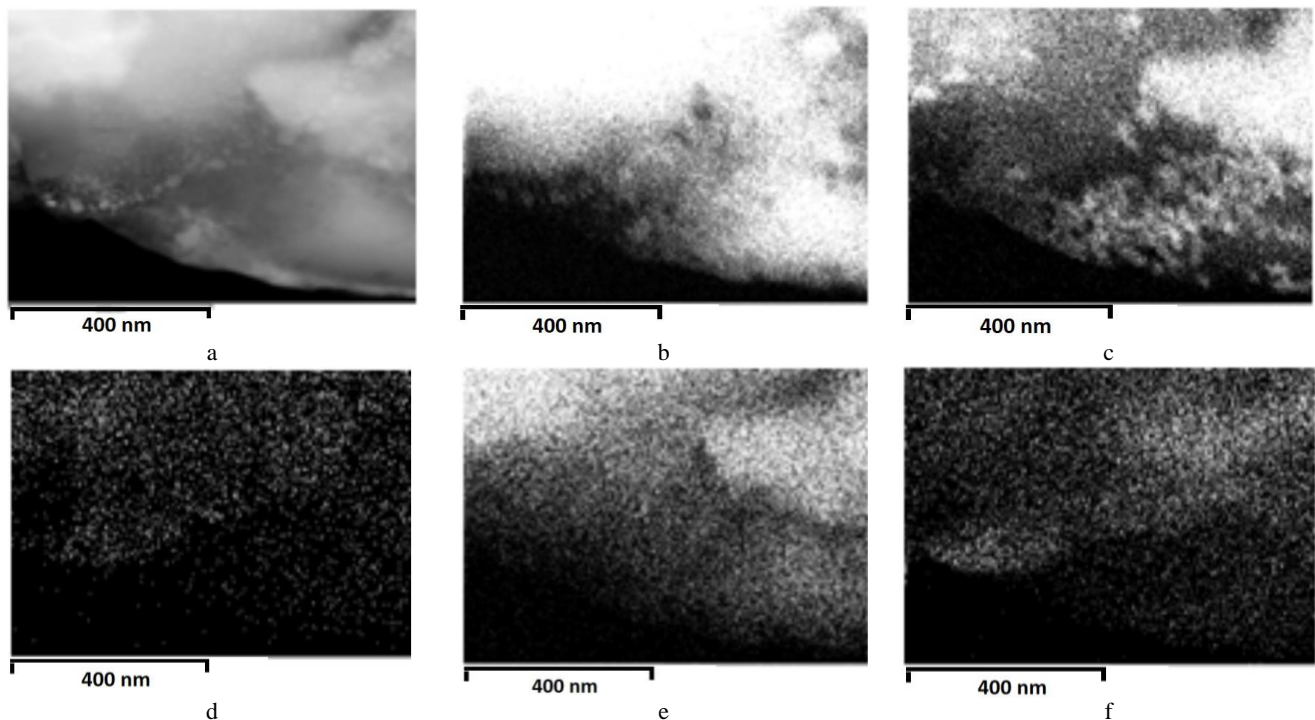


**Fig. 6.** The area for which the analyses have been made and the maps of element distribution in the foil of the Ni-based coating

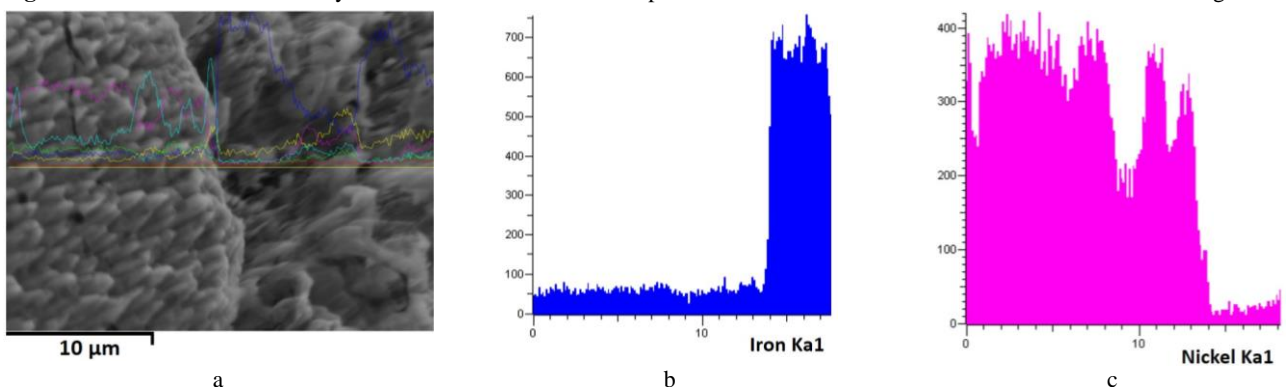


**Fig. 7.** SEM image of microstructure of Ni-based coating (left part of image) on steel substrate (right part of image) with a – line of elements distribution; b – corresponding line of Fe distribution; c – the line of Ni distribution

#### 4. CONCLUSIONS

The irradiation of the coatings by a DC pulse plasma jet according to the recommended in the result of model calculations modes leads to the evolution of the structural-phase state of coatings: the double increase in the size of the diffusion zone between the coating and the substrate,

an increase in the volume fraction of hardening intermetallic phases in average by 5 %, the formation of a sufficiently homogeneous fine-grained structure in the irradiated coatings and, consequently, a significant increase of microhardness (in average on 1 GPa for the Ni-based coatings and on 0.7 GPa for the Co-based coatings), wear resistance (by up to 2–3 times) and corrosion

resistance of modified coatings (the substrate corrosion rate is on average 1.7 times higher). The strengthening particles of intermetallic phases are precipitated in the form of nanosized lamellae. The TEM and SEM observed redistribution of the elements of the coating into the substrate indicates the acceleration of diffusion processes during irradiation (presumably of the radiation-enhanced diffusion).

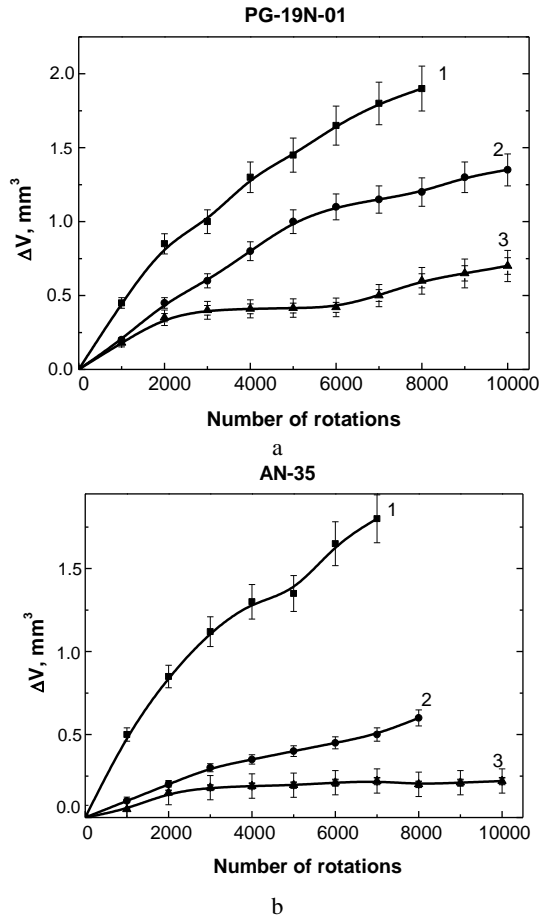


**Fig. 8.** Wear curves obtained on the substrate (1), the initial coatings (2): a – after modification of the powder coatings PG-19N-01; b – and AN-35 by irradiation (3)

### Acknowledgment

This research was funded by the Scientific Committee of the Ministry of Education and Science of the Republic of Kazakhstan for the project “Study of the nanostructures formation in the Ni and Co-based plasma – detonation coatings and search of the science-based exposure modes for coatings modification by irradiation”.

The authors express their gratitude to Prof. Alexander D. Pogrebnjak (Sumy State University, Ukraine) for providing treated samples and support in discussing the results.

### REFERENCES

1. **Pawlowski, L.** The Science and Technology of Thermal Spray Coatings. N. Y., Wiley, 1995: 240 p.
2. **Crawmer, D. E.** Thermal Spray Processes, in: **J.R. Davis (Ed.)**, Handbook of Thermal Spray Technology, ASM International, Materials Park, OH, USA, 2004, pp. 54–84.
3. **Kuroda, S., Kawakita, J., Watanabe, M., Katanoda, H.** Warm Spraying—a Novel Coating Process Based on High-

- Velocity Impact of Solid Particles *Science and Technology of Advanced Materials* 9 (3) 2008: pp. 033002–033004.
4. **Kadyrzhanov, K.K., Komarov, F.F., Pogrebnjak, A.D., Rusaikov, V.S., Turkebaev, T.E.** Ion-beam and Ion-plasma Modification of Materials. M., 2005: 640 p.
5. **Misaelides, P., Hatzidimitou, A., Noli, F., Pogrebnjak, A., Tyurin, Yu., Kosionidis, S.** Preparation, Characterization and Corrosion Behavior of Protection Coatings on Stainless Steel Deposited by Plasma Detonation *Surface and Coatings Technology* 180–181 2004: pp. 290–296.
6. **Barletta, M., Bolelli, G., Bonferroni, B., Lusvardi, L.** Wear and Corrosion Behavior of HVOF-Sprayed WC-CoCr Coatings on Al Alloys *Journal of Thermal Spray Technology* 19 (1–2) 2010: pp. 358–367.
7. **Curry, N., Markocsan, N., Li, X.-H., Tricoire, A., Dorfman, M.** Next Generation Thermal Barrier Coatings for the Gas Turbine Industry *Journal of Thermal Spray Technology* 20 (1–2) 2011: pp. 108–115.
8. **Shiemnev, A. P., Svistunova, G. V.** Corrosion-resistant, Heat-resistant and High-strength Steels and Alloys. M., 2000: pp. 88–102.
9. **Friend, W. Z.** Corrosion of Nickel and Alloys. N.Y., 1980: pp. 164–170.
10. **Svistunova, T. V.** Corrosion-resistant Alloys for Highly Aggressive Environments *Metal Science and Heat Treatment* 8 2005: pp. 36–42.
11. **Smithells, C. I.** Metals Reference Book. Translated from English. M., 1980: pp. 224–241.
12. **Burns, R.M., Bradley, W.W.** Protective Coatings for Metals. N. Y., 1967: pp. 37–43.
13. **Ivanov, Yu. F., Nadeikin, E. V.** Structure and Properties of Coatings Created by Plasma Deposition Technique and Treated by Electron-Beam *Russian Physics Journal* 8/2 2009: pp. 402–404.
14. **Alontseva, D., Pogrebnjak, A., Kolesnikova, T., Russakova, A.** Modeling of Processes in Co-Based Coatings Exposed to Plasma Jet Irradiation *Materials Science (Medziagotyra)* 19 3 2011: pp. 277–282.
15. **Alontseva, D. L., Pogrebnjak, A. D., Klassen, G.** The Structure-Phase Compositions of Ni–Cr and Co–Cr Based Powder Alloys Coatings Deposited by Plasma-Detonation on Steel Substrates *Thirteenth International Conference on Plasma Surface Engineering* 2012: pp. 447–450.
16. **Alontseva, D., Russakova, A.** The Structure-Phase Compositions and Properties of Plasma-Detonation Ni and Co-Based Powder Alloys Coatings *Advanced Materials Research* 702 2013: pp. 94–99.
17. **Alontseva, D., Krasavin, A., Pogrebnjak, A., Russakova, A.** Modification of Ni-Based Plasma Detonation Coatings by a Low-Energy DC E-beam *Acta Physica Polonica A* 123 5 2013: pp. 867–870.
18. **Westbrook, J. H., Fleischer, R. L.** Intermetallic Compounds, Principles and Practice. England, 1994: p. 1934.
19. **Kurzina, I.A., Kozlov, E.V., Sharkeev, Yu.P.** Nanocrystalline intermetallic and Nitride Structures Formed During Ion-Beam Exposure. Tomsk, 2008: p. 324.
20. **Sukhovarov, V. F.** The Cellular Precipitation in Alloys. N., 1983: 112–130.
21. **Basak, A. K., Matteazzi, P., Vardavoulias, M., Celis, J.-P.** Corrosion–wear behavior of thermal sprayed nanostructured FeCu/WC–Co coatings *Wear* 261 2006: pp. 1042–1050.
22. **Zazi, N.** Effect of Heat Treatments on The Microstructure, Hardness and Corrosion Behavior of Nondendritic ALSi<sub>9</sub>Cu<sub>3</sub>(Fe) Cast Alloy *Materials Science (Medziagotyra)* 19 3 2011: pp. 258–269.
23. **Nolfi, F. V.** Phase Transformation during Irradiation. Chelyabinsk, 1989: 228–246.